The quandary of detecting the signature of climate change in Antarctica

Mathieu Casado, Raphaël Hébert, Davide Faranda, Amaelle Landais

The quandary of detecting the signature of climate change in Antarctica

Mathieu Casado[1,*], Raphael Hébert[2], Davide Faranda[1,3,4], and Amaelle Landais[1]

[1]Laboratoire des Sciences du Climat et de l'Environnement, UMR 8212 CEA-CNRS-UVSQ, Université Paris-Saclay, IPSL, 91191 Gif-sur-Yvette, France
[2]Alfred Wegener Institut Helmholtz Centre for Polar and Marine Research, Potsdam, Germany,
[3]London Mathematical Laboratory, 8 Margravine Gardens London, W6 8RH, UK
[4]LMD/IPSL, Ecole Normale Superieure, PSL research University, Paris, France
[*]Correspondence to: mathieu.casado@gmail.com

ABSTRACT

Global warming driven by human activities is expected to be accentuated in Polar Regions compared to the global average, an effect called the polar amplification. Yet, for Antarctica, the amplitude of warming is still poorly constrained due to short weather observations and the large decadal climate variability. Using a compilation of 78 ice core records, we provide a high-resolution reconstruction of past temperatures over the last 1000 years for seven regions of Antarctica and direct evidence of Antarctic polar amplification at regional and continental scales. We also show that the amplitude of both natural and forced variability is not captured by the CMIP5 and 6 model ensemble members, part of which could be explained by the Southern Annular Mode (SAM). This shows that not considering feedback loops causing the polar amplification could lead to an underestimation of the magnitude of anthropogenic warming and its consequences in Antarctica.

Mean surface air temperature (SAT) has been globally increasing over the last century[1,2] due to anthropogenic greenhouse gas emissions, reaching warming levels beyond natural variability[3]. Polar Regions are expected to be impacted by larger temperature increases than the global average due to the polar amplification[4]. Polar amplification, while well established in the Arctic[5,6], is only anecdotally reported in Antarctica[7–9] and expected to be smaller than its Arctic counterpart[10,11]. At the continental scale, the signature of anthropogenic climate change over the last decades has been detected[9] but not consistently identified nor quantified in observations[12], because of sparse available temperature records[13] and the large impact of internal variability in Antarctica[14], in particular the decadal signature of the SAM[15]. In addition, the onset of the anthropogenic warming could be delayed in the southern high latitudes[1,16]. This strongly differs from climate models which suggest a detectable anthropogenic warming at the continental scale in Antarctica[1,17], while so far, a significant anthropogenic warming has only been detected in West Antarctica and the Antarctic Peninsula[18,19]. On the other hand, little change is observed in East Antarctica[13,20], clouded by the natural variability and the signature of SAM[15]. As a result, the decadal variability complicates the detection of a multi-decadal forced warming trend[21].

Due to the absence of weather stations in Antarctica covering periods longer than 60 years[22], water isotopes from ice core records provide one of the best archives of past temperature variability over the last millennia[23]. The link between water isotopic composition (δD and $\delta^{18}O$) and temperature derives from the progressive depletion of heavy isotopes in precipitation during the distillation of atmospheric water masses travelling toward colder regions. There are two main challenges regarding the interpretation of the water isotopic signal as a temperature proxy: the conversion from isotopic composition to temperature[24,25] and the recording of the signal during archival processes[26,27]. By averaging enough records, Münch et al[28] showed that a meaningful climate record can be obtained from interannual timescales, even over the central Plateau Regions of Antarctica where low accumulations exacerbate the impact of archival processes on the isotopic signal. By stacking together a large number of records across Antarctica, Stenni et al[29] inferred past temperature variability and trends over the last 1000 years in Antarctica, but fell short of identifying a significant anthropogenic warming trend for all of Antarctica, or even regionally for East Antarctica. We suggest that the failure to detect a clear warming trend in Antarctica is due to relatively large natural variability, overshadowing the forced response[17,30]. In order to separate natural and forced variability, which are of similar magnitudes[31], advanced statistical analyses guided by physical intuition are necessary. We make use of persistence metrics rooted in dynamical systems theory that are locally defined in the phase space of the analysed variables, and thus sensitive to all intrinsic timescales involved in the dynamics, such as changes induced by non-stationary forcing[32]. As a result, persistence metrics are robust with respect to featureless noisy components and can be used to detect a change of regime in noisy systems such as the North Atlantic mid-latitude atmospheric dynamics[33], or ocean dynamics[34].

Here, we make use of 78 water isotopic records from Antarctica from the Iso2k database[35] to generate time series of past isotopic compositions (referred to as the iso2k stack) with sufficient length and resolution to allow detection of the emergence of anthropogenic climate change in the context of the last 1000 years for seven regions of Antarctica (see Methods), as well as for all of Antarctica (referred to as Pan-Antarctica). The network of ice cores used here captures about 70% of the variance of the Pan-Antarctica average temperature variations (Supplementary Section S9). The persistence discerns changes in the dynamical structure of multi-decadal climate variability, while the spectral analysis quantifies the signal-to-noise ratio as a function of timescale in the stacks of ice core records. Together, these approaches allow us to build a comprehensive picture of climate variability across timescales for Antarctica using the ice core data, instrumental data, and model simulations.

Detecting a warming signal in noisy records

Trend estimators may not be sufficient to detect anthropogenic warming at the regional scale where natural variability is large[36], as they are inherently constrained by the choice of the window length (Extended Data Figure ED1,

Supplementary Section S5) and by the characteristics of the residuals. When natural variability has positive temporal autocorrelation (akin to red noise), its phase can lead to a large spread in trend estimates for short windows (see Fig. 1 a), or biases for long windows encompassing periods before the trend started, thus diluting the trend. For instance, moving trends calculated on the iso2k ice core stack with windows of 40 years (Fig. 2d) do not show a significant warming trend with respect to the last 1000 years, likely because of the natural variability. In contrast, the 100-year window length used by Stenni et al[29] may have underestimated the recent warming trend, as it included a period where the anthropogenic forcing was still weak (Extended Data Figure ED1). For both the iso2k stack and Stenni et al[29], we show that a window length of 50 years minimises both of these effects and leads to the detection of a warming trend (Extended Data Figure ED1), albeit with large error bars.

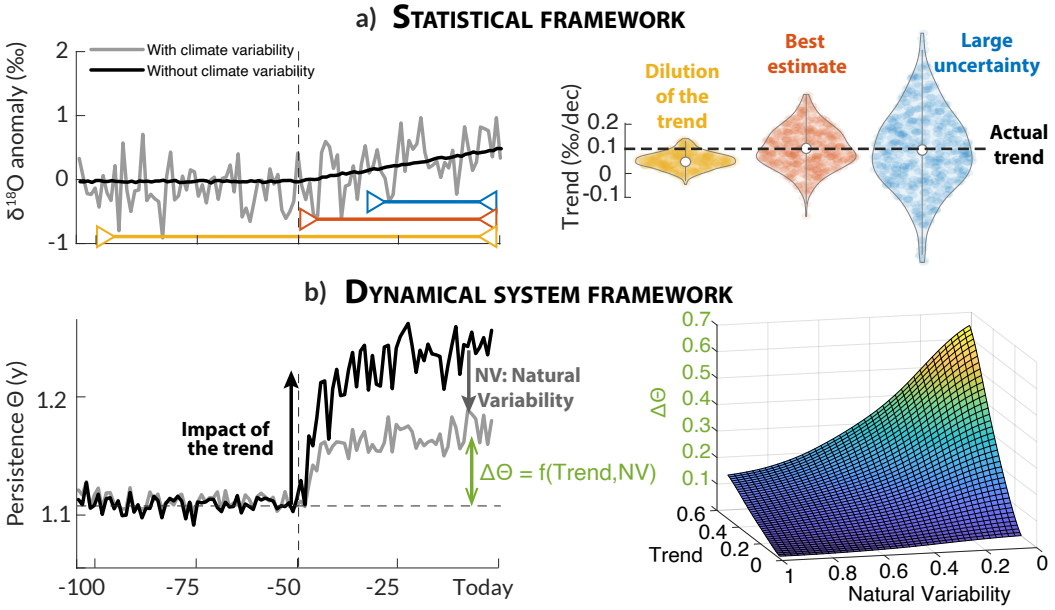

Figure 1. Quantification of the impact of climate change in Antarctica when a large amount of natural variability competes with the warming signal: a) application of the statistical framework for trend estimates on, left, surrogate time series of isotopic composition with (grey line) and without (black line) natural variability and a warming trend starting -50 years before today and, right, estimates of the trend from an ensemble of 2500 time series with natural variability for window lengths of 30, 50 and 100 years; the trend estimate is strongly affected by the choice of the window over which the trend is calculated, leading to large uncertainty for small windows and biases for long windows, b) application of the dynamical system theory to the same time series: left, persistence Θ calculated on the surrogate data, and right, 3D surface of the changes of persistence induced by a trend for various amount of natural variability. The latter approach can be a powerful way to quantify the warming trend for situations where the amplitude of the trend is of the same order of magnitude than the amplitude of the natural variability.

Here, we make use of a persistence metric to detect changes in the dynamics underlying the $\delta^{18}O$ timeseries[37] (See Methods). Numerical experiments show that under realistic assumptions (spectra matching that of ice core records, see Extended Data Figures ED2 and ED3), the change of persistence ($\Delta\Theta$) directly relates to the amplitude

of the trend (positive relationship) and the natural variability (negative relationship, see Extended Data Figure ED4).

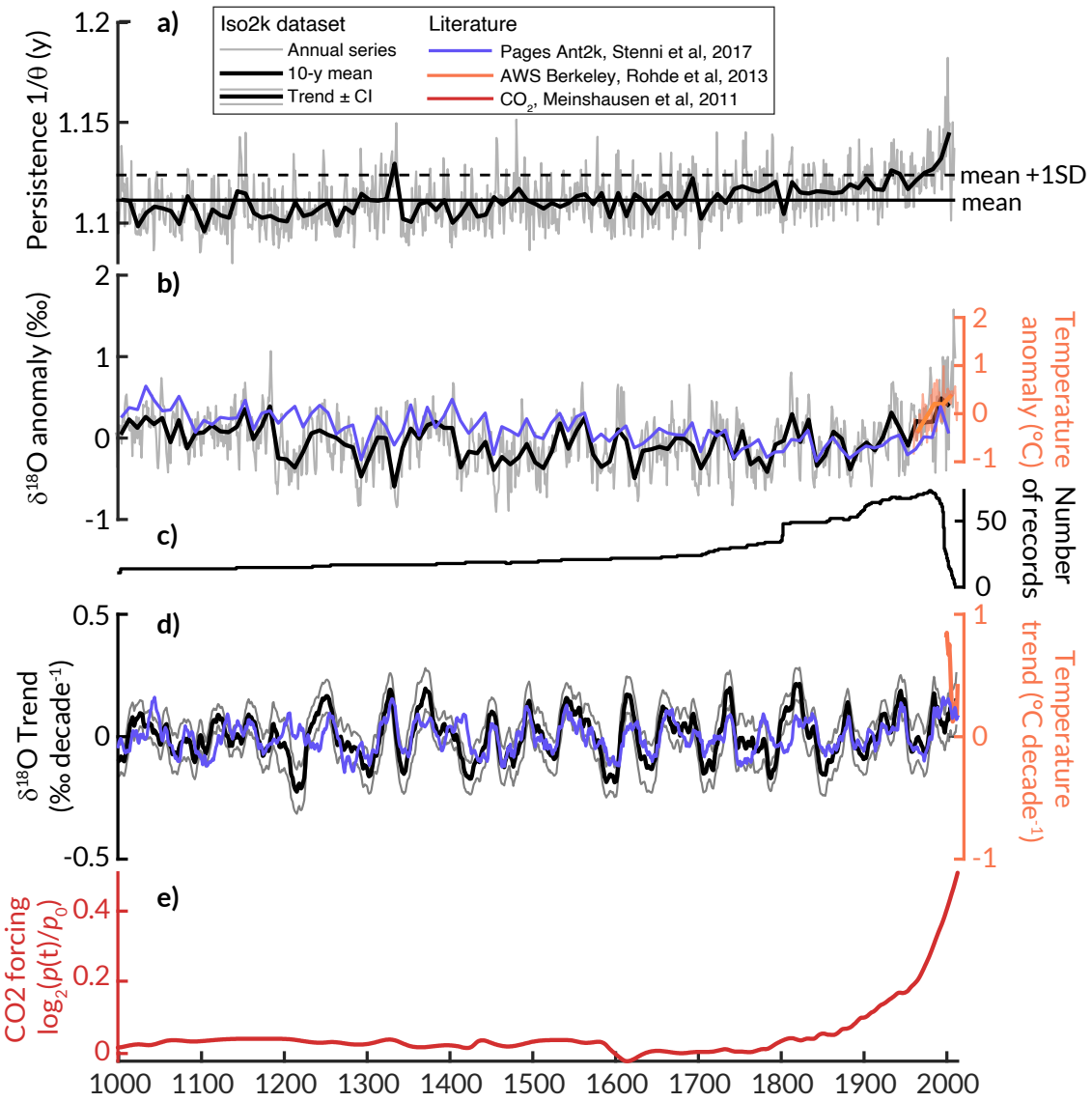

Figure 2. Identifying the signature of climate change in Antarctica in the context of the last 1000 years: a) time series of the persistence metric (Θ, y), b) isotopic composition anomaly stack for all ice cores in Antarctica (in δ^{18}O units ‰), compared to the previous stack realised by Stenni et al[29] (‰), instrumental temperature measurements (°C, see Methods), c) number of records covering a given time period , d) trend on 40-year running windows ending on the given year with confidence intervals, and e) CO_2 forcing[38]. For θ and δ^{18}O, light grey curves are the original data with annual resolution, thick black curves are 10-year block averages. Note that the block averages and the trend estimates do not take into account datapoints after 2008 when the number of available cores drop below 10. For the top panel, the horizontal solid line represents the average value, while the horizontal dashed line is the average value +1 std.

Using the iso2k stack, we performed estimates of Θ for the last 1000 years (Fig. 2). Overall, during the

pre-industrial period, the average value of Θ (around 1.1 year) is significantly higher ($p<0.05$) than expected for a diffused white noise (around 1.06 for typical ice core diffusion values), confirming that the stacked record contains a persistent red noise signal, in line with the expected characteristics of a climate signal[39–41]. Increasing values of Θ over the last century (reaching more than 1.15 in 2000) indicates a change of dynamical properties unprecedented in the 1000-year record ($p<0.01$, Fig. 2 and Fig. ED7). We observe similar behaviour with increased values of Θ for the East Antarctic Plateau, West Antarctica, Victoria Land, and the Indian Coast regions (Extended Data Figure ED5).

In order to evaluate if this change in the dynamical properties is related to anthropogenic forcing, we compare the time series of isotopic composition and persistence with the CO_2 concentration. The link between the observed changes in isotopic composition (and thus of temperature) and the increase in CO_2 concentration is relatively weak ($r^2 = 0.4$ between 1800 and 2000, $p<0.05$), especially compared to what is observed for global temperature and high-latitude land regions in the Northern Hemisphere[42]. In contrast, the change of persistence follows the change of CO_2 forcing much more closely ($r^2 = 0.8$ between 1800 and 2000, $p<0.05$), suggesting that greenhouse gas concentration may be the cause for the observed changes in dynamical properties of Antarctic temperatures.

Estimating the ratio between natural and forced variability

Converting changes in isotopic composition to temperature is an arduous task[25,43]. Consequently, the ice core community sometimes avoids the conversion to temperature when discussing climate variability[29]. Here, we convert the trends obtained from the iso2k stack into temperature using a spectral approach (Extended Data Figure ED6, and Methods). The pan-Antarctic isotopic trend estimates for the 1950-2005 period (0.11 ± 0.02‰/dec) can thus be converted to a temperature trend of 0.22 ± 0.04 °C/dec (Fig. 3), compared to 0.25°C/dec in ERA5, 0.18 ± 0.07 °C/dec in the CMIP5 P1000 ensemble models (n = 9, see Supplementary Section S7), and 0.11 to 0.18°C/dec in weather station derived observations[13,15]. As the mean global temperature warming trend is evaluated between 0.14 and 0.18°C/dec[3], this warming suggest the presence of an Antarctic Amplification. Similarly, at the regional scale, trend estimates from the iso2k ice core stack, ERA5, and CMIP5 models seem to yield matching amplitudes for East Antarctica, larger amplitudes in the ice cores and ERA5 than in CMIP5 for the Antarctic Peninsula, West Antarctica and Dronning Maud Land coast, and larger amplitudes in ERA5 than in the ice cores and CMIP5 for Weddell Coast and Victoria Land.

In the dynamical system framework, for the Pan-Antarctic stack over the same period (1950 - 2005), we observe that the increase in persistence is much larger in the isotope series (0.026 y) and ERA5 (0.018 y) than in the CMIP5 outputs (0.007 ± 0.007 y, where the uncertainty indicates the spread of the ensemble). The underestimation of the change in persistence in the model simulations can be attributed to either larger warming trends in observations

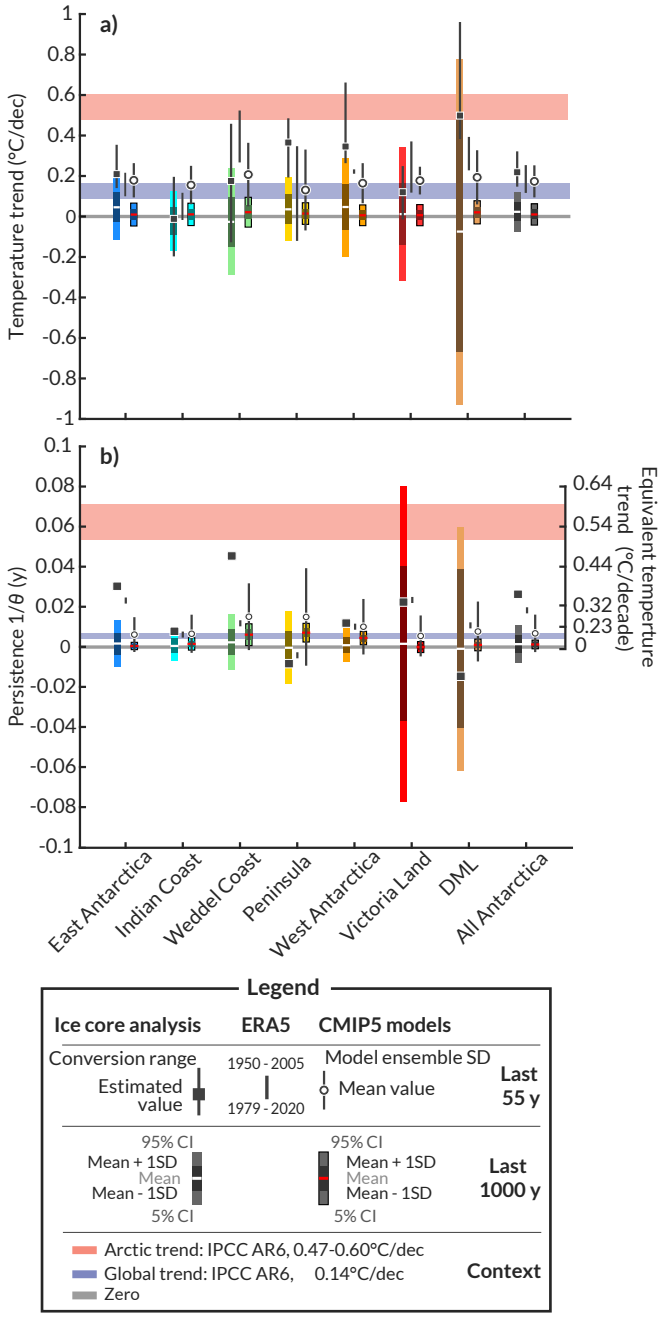

Figure 3. The current climate change in Antarctica in the context of the last 1000 years: a) temperature trend, and b) persistence values found for the last 55 years on record (1950 to 2005) (dark square, spectral calibration of isotope-temperature slope, and bar, range of calibration from the literature, see Methods) compared to the confidence interval for the last 1000 years found from the ice core data for each regions, as well as compared to the trend and persistence found in ERA5 and in the CMIP5 P1000 ensemble members. The error bars for the trend estimates (panel a) include both the uncertainty of the isotope to temperature conversion (Extended Data ED6, see Methods), and the simulated uncertainty on trend estimates for the given window length (Extended Data ED1, see Methods). For ERA5, the range of values provided corresponds to the trend from 1979 to 2020 (lower value of the bar) and 1950 to 2005 (higher value of the bar).

than in the models, or stronger natural variability in CMIP5 models than in the observations. The latter is not supported by spectral analyses of the CMIP5 model simulation showing an underestimation of the decadal and multi-decadal variability compared to ERA5 and ice core records[44]. As a result, the changes in persistence suggest, independently of the isotope-temperature calibration, that the warming trend must be significantly larger in the ice core reconstructions than in the CMIP5 models. The observed change of Θ (0.026 y) can be directly converted into a warming trend for reasonable assumptions of the natural variability amount (e.g. power-law noise with $\beta = 0.6$ and decadal natural variability of 0.6 ‰²y, see Methods). This dynamical estimator (as opposed to a statistical trend estimator) suggests a warming trend of 0.16 ± 0.04 ‰/dec (equivalent to [0.32 - 0.45]°C/dec with the most likely conversion factor, see Methods), which is larger than the direct measurement of the trend (0.11 ± 0.02 ‰/dec), suggesting that the latter is possibly underestimating the magnitude of climate change in Antarctica due to the impact of natural variability (Extended Data Figure ED1, and Supplementary Section S11).

At the regional scale, the persistence approach identifies similarly large amplitudes of warming for East Antarctica (0.18 ‰/dec), Weddell Coast (0.18 ‰/dec), and Victoria Land (0.17 ‰/dec), three times larger than what is obtained from CMIP5 models for these three regions where the warming is limited to 0.10°C/dec, and thus less than 0.05 ‰/dec. Interestingly, for West Antarctica, where the iso2k stack estimates a warming trend (0.24 ‰/dec, equivalent to ≈ 0.34°C/dec) much larger than ERA5 and the CMIP5 ensemble (0.24 and 0.17 ± 0.10°C/dec, respectively), the persistence change obtained for both the iso2k stack and CMIP5 model outputs suggests a similar increase of 0.011y, equivalent to a warming of roughly 0.26°C/dec, in good agreement with ERA5 recorded warming. This suggests that the warming trend obtained with traditional statistical approaches (0.32°C/dec) is conflated by a positive contribution of the natural and forced variability (for instance the SAM), to which the persistence diagnostic is less sensitive to than trends (Supplementary Section S5). The dynamical system framework predicts a warming trend for West Antarctica (0.26°C/dec), in line with the literature (around 0.20°C/dec)[13,19,20]. In the case of the Antarctic Peninsula, the small number of records before 1875 leads to a very noisy persistence estimate (Fig. ED5a), and the analysis is inconclusive.

Overall, trends in the statistical framework (Fig. 3 a)) suggest the presence of a polar amplification underestimated by CMIP5 models for most regions of Antarctica (including Pan Antarctica). The persistence provides calibration-free evidence that the magnitude of the current climate change is underestimated by CMIP5 models across Antarctica. It also suggests that the amplitude of the natural variability in the CMIP5 models is underestimated, which could also be linked to an inadequate integration of polar amplification in CMIP5 models. Both approaches used here to evaluate the warming trends are complementary to detection-attribution methods, which combine observations and model simulations with different forcings (in particular for greenhouse gases). While detection-attribution

methods showed a warming mostly in West Antarctica and the Antarctic Peninsula[19,20], the Iso2k ice core stack detects a large warming in East Antarctica as well. Weather station records also support a limited warming in East Antarctica[13], except for anecdotal reports of warming at South Pole and Vostok stations[8], notably due to SAM congruent cooling trends[15].

Reconciling the model-observation discrepancies

To evaluate the link between how climate models underestimate the anthropogenic warming trend and the natural variability in Antarctica, we study the discrepancies between the anthropogenic warming and natural variability predicted by CMIP5 and CMIP6 ensemble models and the observations obtained from ice core records, ERA5, and weather stations (See Methods). In the model simulations, we observe a weak ($r = 0.38$) but significant relationship ($p < 0.01$) between the amplitudes of the modelled warming trend induced by climate change and the amplitudes of natural decadal variability (Fig. 4), confirming the link between the underestimation of the anthropogenic warming and of the natural variability[45,46]. The relationship is naturally very clear when comparing the decadal forced variability to the warming trends ($r = 0.69$, $p < 0.001$), or the decadal forced variability ratio to the natural variability ratio ($r = 0.83$, $p < 0.001$). Ice core records in Antarctica thus confirm that CMIP5 past1000 and CMIP6 historical simulations alike underestimate both the anthropogenic warming (Kruskal-Wallis ANOVA test, $p < 0.05$), and the multi-decadal temperature variability, in line with what was already observed for marine[40] and for terrestrial records[41]. ERA5, which compares well with the ice core estimates from 1950 to 2005, presents a potential discontinuity around 1979, the date when satellite data starts to be widely assimilated. While the temperature change could be linked to changes in atmospheric circulation[47], the warming trend in ERA5 (1950-2005: 0.25°C/dec) is much larger than in weather station observations (0.08°C/dec)[15] or when taking into account the period from 1979 to 2020 in ERA5 (0.14°C/dec).

The negative contribution of the SAM to the Antarctic warming trends from 1979 partly explains the difference between the trends observed in weather stations and climate models[15,47]. It is also likely having an influence on the climatic signal recorded by water isotopes in ice core records, and could explain part of the difference observed between the trends in the iso2k stack and CMIP5 and 6 model outputs. Indeed, as an integrated tracer of the hydrological cycle, ice core isotopic composition records of the temperature are modulated by the precipitation intermittency and the history of the air masses towards ice core location[48]. Largest snowfall events are associated with synoptic events often characterised by a negative phase of SAM[49,50]. It was observed at Dome F and Aurora Bassin North that SAM- influences the deposited snow $\delta^{18}O$ because large snowfall events occur in winter during warm synoptic events hence contributing with relatively high precipitation $\delta^{18}O$[49,50]. As a result, if the deposited snow $\delta^{18}O$ in Antarctica is always dominated at first order by SAM- phases, the SAM congruent trend should

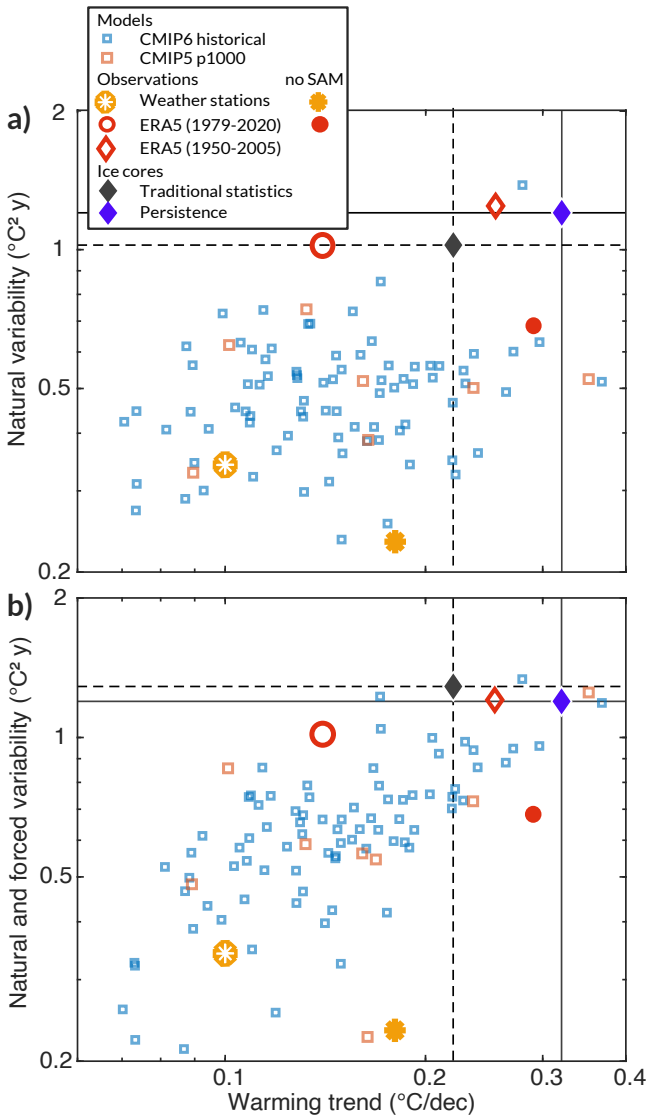

Figure 4. Decadal variability recorded as a function of the observed warming trend: ice cores predictions from both the statistical and dynamical system framework (0.22 and 0.32°C/dec, respectively, obtained with the most likely isotope to temperature conversion, 0.5‰/°C) vs the simulated warming trend by CMIP5 and CMIP6 model ensembles, as well as observations from weather stations[13], and ERA5 outputs : a) decadal variability (5 - 40 years) limited to natural variability (obtained from a detrended spectrum between 1820 and 1900), and b) decadal variability including both natural and forced variability (obtained from a non-detrended spectrum between 1920 and 2005). The trends for the iso2k stack and the models were computed from 1950 to 2005. We include ERA5 trend values for both the 1950-2005 and 1979-2020 windows for comparison purposes with the iso2k stack and weather stations, respectively. For the observations from weather forecast and from ERA5, we evaluated on the most recent time window (1979 to 2020) the background warming trend and variability[15] (without the SAM congruent trend, full circle/asterisk) (see Supplementary Section S11).

not be visible in the water isotopic record which should then be an indicator of the background temperature. The isotopic signal recorded in ice core records could be biased toward the background temperature variations (see Supplementary Section S11), rather than the actual average temperature variations. The iso2k stack record warming

(0.22 - 0.32°C/dec) would then be in agreement with the background warming from CMIP model ensembles (0.28°C/dec), suggesting that the changes of atmospheric circulation could partly explain the difference between model predictions and estimates from the iso2k stack. These results highlight the complex links between forced and natural variability, and that the accuracy of climate projections rely on understanding these links. Indeed, future projections of the SAM, in the context of climate change and recovery of the ozone layer[51], will determine if the SAM will continue to mitigate warming in Antarctica[15].

In Antarctica, the weak anthropogenic warming in model simulations indicates that the multiple feedback loops contributing to the Polar Amplification in Antarctica may not be adequately represented, and that model simulations generally show weaker than expected anthropogenic warming for the same reason that they produce smaller than expected natural variability[15,52]. As the power law scaling obtained for the spectrum of climate model outputs (using a red noise to describe the climate power spectral density) are lower than observed ones in Antarctica[28,44], this suggests that natural (internal) variability is misrepresented[40]. Tropical teleconnections play an important role in driving Antarctic natural variability, especially in West Antarctica[53,54], and the underestimation of variability by climate models may thus be related to challenges in simulating multi-decadal modes of variability in tropical sea-surface temperature[55]. In the Arctic, similar predictions that CMIP5 and CMIP6 models alike underestimate both the amplitude of the anthropogenic warming[6] and the natural variability[56] imply as well that the cause of the Arctic Amplification is being misrepresented. It remains a challenge to improve the performances of simulated local and regional variability while preserving the performance of current climate models at the global scale[57].

Conclusion

Anthropogenic warming in Antarctica, in particular in the interior of the continent, has been obscured by both the large natural variability[8] and the lack of observations or unbiased proxy records[29]. The historical context of the past temperature changes provides a null hypothesis over which the anthropogenic climate change can be identified. Separating the anthropogenic warming from the natural variability in Antarctica highlighted the profound mismatch between models and observations. Our results suggest that climate models underestimate the impact of polar amplification on both the natural variability and magnitude of the anthropogenic warming, which is key for future scenarios to predict Antarctic warming, and for detection-attribution of the current observed changes. For instance, the potentially enormous contribution to sea level rise of the Antarctic Peninsula and West Antarctica[58] would be strongly affected by the twofold underestimation of warming in these regions[59].

Here, the paleoclimate, statistics, and modeling communities should work together to reconcile the model-data mismatch on the polar amplification. A more complete network of ice cores in Antarctica would provide a better

constraint on local variability that would contribute to a more complete representation in global climate models of the various feedback loops causing the natural and forced variability in Antarctica.

References

1. Abram, N. J. *et al.* Early onset of industrial-era warming across the oceans and continents. *Nature* **536**, 411–418 (2016).
2. Sippel, S., Meinshausen, N., Fischer, E. M., Székely, E. & Knutti, R. Climate change now detectable from any single day of weather at global scale. *Nat. Clim. Chang.* **10**, 35–41, DOI: 10.1038/s41558-019-0666-7 (2020).
3. IPCC, Masson-Delmotte, V., P. Zhai, A. Pirani, S., L. Connors, C. Péan, S. Berger, N. Caud, Y. Chen, L. Goldfarb, M. I. Gomis, M. Huang, K. Leitzell, E. Lonnoy, J. B., R. Matthews, T. K. Maycock, T. Waterfield, O. Yelekçi, R. Y. & Zhou, B. Climate Change 2021: The Physical Science Basis. Contribution of Working Group I to the Sixth Assessment Report of the Intergovernmental Panel on Climate Change. Tech. Rep. (2021).
4. Manabe, S. & Wetherald, R. T. The effects of doubling the CO2 concentration on the climate of a general circulation model. *J. Atmospheric Sci.* **32**, 3–15 (1975).
5. Bekryaev, R. V., Polyakov, I. V. & Alexeev, V. A. Role of Polar Amplification in Long-Term Surface Air Temperature Variations and Modern Arctic Warming. *J. Clim.* **23**, 3888–3906, DOI: 10.1175/2010JCLI3297.1 (2010).
6. Rantanen, M. *et al.* The Arctic has warmed nearly four times faster than the globe since 1979. *Commun. Earth Environ.* **3**, 168, DOI: 10.1038/s43247-022-00498-3 (2022).
7. Lazzara, M. A., Keller, L. M., Markle, T. & Gallagher, J. Fifty-year Amundsen-Scott South Pole station surface climatology. *Atmospheric Res.* **118**, 240–259, DOI: http://dx.doi.org/10.1016/j.atmosres.2012.06.027 (2012).
8. Clem, K. R. *et al.* Record warming at the South Pole during the past three decades. *Nat. Clim. Chang.* **10**, 762–770 (2020).
9. Gillett, N. P. *et al.* Attribution of polar warming to human influence. *Nat. Geosci.* **1**, 750–754, DOI: 10.1038/ngeo338 (2008).
10. Salzmann, M. The polar amplification asymmetry: role of Antarctic surface height. *Earth Syst. Dynam.* **8**, 323–336, DOI: 10.5194/esd-8-323-2017 (2017).
11. Hahn, L. C. *et al.* Antarctic Elevation Drives Hemispheric Asymmetry in Polar Lapse Rate Climatology and Feedback. *Geophys. Res. Lett.* **47**, e2020GL088965, DOI: https://doi.org/10.1029/2020GL088965 (2020).
12. Stenni, B. *et al.* Three-year monitoring of stable isotopes of precipitation at Concordia Station, East Antarctica. *The Cryosphere* **2016**, 1–30, DOI: 10.5194/tc-2016-142 (2016).

13. Nicolas, J. P. & Bromwich, D. H. New Reconstruction of Antarctic Near-Surface Temperatures: Multidecadal Trends and Reliability of Global Reanalyses. *J. Clim.* **27**, 8070–8093, DOI: doi:10.1175/JCLI-D-13-00733.1 (2014).

14. England, M. R. Are Multi-Decadal Fluctuations in Arctic and Antarctic Surface Temperatures a Forced Response to Anthropogenic Emissions or Part of Internal Climate Variability? *Geophys. Res. Lett.* **48**, e2020GL090631 (2021).

15. Jones, M. E. *et al.* Sixty Years of Widespread Warming in the Southern Middle and High Latitudes (1957–2016). *J. Clim.* **32**, 6875–6898, DOI: 10.1175/JCLI-D-18-0565.1 (2019).

16. Armour, K. C., Marshall, J., Scott, J. R., Donohoe, A. & Newsom, E. R. Southern Ocean warming delayed by circumpolar upwelling and equatorward transport. *Nat. Geosci.* **9**, 549–554, DOI: 10.1038/ngeo2731 (2016).

17. Jones, J. M. *et al.* Assessing recent trends in high-latitude Southern Hemisphere surface climate. *Nat. Clim. Chang.* **6**, 917–926, DOI: 10.1038/nclimate3103 (2016).

18. Schneider, D. P. & Steig, E. J. Ice cores record significant 1940s Antarctic warmth related to tropical climate variability. *Proc. Natl. Acad. Sci.* **105**, 12154–12158 (2008).

19. Dalaiden, Q., Schurer, A. P., Kirchmeier-Young, M. C., Goosse, H. & Hegerl, G. C. West Antarctic Surface Climate Changes Since the Mid-20th Century Driven by Anthropogenic Forcing. *Geophys. Res. Lett.* **49**, e2022GL099543 (2022).

20. Steig, E. J. *et al.* Warming of the Antarctic ice-sheet surface since the 1957 International Geophysical Year. *Nature* **457**, 459–462 (2009).

21. Von Storch, H. *et al.* Reconstructing past climate from noisy data. *Science* **306**, 679–682 (2004).

22. Turner, J. *et al.* The SCAR READER project: toward a high-quality database of mean Antarctic meteorological observations. *J. Clim.* **17**, 2890–2898 (2004).

23. Jouzel, J. & Masson-Delmotte, V. Paleoclimates: what do we learn from deep ice cores? *Wiley Interdiscip. Rev. Clim. Chang.* **1**, 654–669, DOI: 10.1002/wcc.72 (2010).

24. Jouzel, J. *et al.* Magnitude of isotope/temperature scaling for interpretation of central Antarctic ice cores. *J. Geophys. Res. Atmospheres* **108** (2003).

25. Klein, F. *et al.* Assessing the robustness of Antarctic temperature reconstructions over the past 2 millennia using pseudoproxy and data assimilation experiments. *Clim. Past* **15**, 661–684, DOI: 10.5194/cp-15-661-2019 (2019).

26. Casado, M. *et al.* Archival processes of the water stable isotope signal in East Antarctic ice cores. *The Cryosphere* **12**, 1745–1766, DOI: 10.5194/tc-12-1745-2018 (2018).

27. Laepple, T. *et al.* On the similarity and apparent cycles of isotopic variations in East Antarctic snow pits. *The Cryosphere* **12**, 169–187, DOI: 10.5194/tc-12-169-2018 (2018).

28. Münch, T. & Laepple, T. What climate signal is contained in decadal-to centennial-scale isotope variations from Antarctic ice cores? *Clim. Past* **14**, 2053–2070 (2018).

29. Stenni, B. *et al.* Antarctic climate variability on regional and continental scales over the last 2000 years. *Clim. Past* **13**, 1609–1634 (2017).

30. Franzke, C. A novel method to test for significant trends in extreme values in serially dependent time series. *Geophys. Res. Lett.* **40**, 1391–1395, DOI: https://doi.org/10.1002/grl.50301 (2013).

31. Goosse, H., Renssen, H., Timmermann, A. & Bradley, R. S. Internal and forced climate variability during the last millennium: a model-data comparison using ensemble simulations. *Quat. Sci. Rev.* **24**, 1345–1360 (2005).

32. Faranda, D., Freitas, J. M., Lucarini, V., Turchetti, G. & Vaienti, S. Extreme value statistics for dynamical systems with noise. *Nonlinearity* **26**, 2597–2622, DOI: 10.1088/0951-7715/26/9/2597 (2013).

33. Faranda, D., Alvarez-Castro, M. C., Messori, G., Rodrigues, D. & Yiou, P. The hammam effect or how a warm ocean enhances large scale atmospheric predictability. *Nat. communications* **10**, 1–7 (2019).

34. Giamalaki, K. *et al.* Future intensification of extreme Aleutian low events and their climate impacts. *Sci. reports* **11**, 1–12 (2021).

35. Konecky, B. L. *et al.* The Iso2k Database: A global compilation of paleo-δ18O and δ2H records to aid understanding of Common Era climate. *Earth Syst. Sci. Data* (2020).

36. Rodionov, S. N. The problem of red noise in climate regime shift detection. *Geophys. Res. Lett.* **31**, L12707 (2006).

37. Lucarini, V. *et al. Extremes and recurrence in dynamical systems* (John Wiley I& Sons, 2016).

38. Meinshausen, M. *et al.* The RCP greenhouse gas concentrations and their extensions from 1765 to 2300. *Clim. Chang.* **109**, 213, DOI: 10.1007/s10584-011-0156-z (2011).

39. Huybers, P. & Curry, W. Links between annual, Milankovitch and continuum temperature variability. *Nature* **441**, 329–332 (2006).

40. Laepple, T. & Huybers, P. Ocean surface temperature variability: Large model–data differences at decadal and longer periods. *Proc. Natl. Acad. Sci.* **111**, 16682–16687, DOI: 10.1073/pnas.1412077111 (2014).

41. Hébert, R., Herzschuh, U. & Laepple, T. Millennial-scale climate variability over land overprinted by ocean temperature fluctuations. *Nat. geoscience* DOI: 10.1038/s41561-022-01056-4 (2022).

42. Hébert, R. & Lovejoy, S. Regional Climate Sensitivity- and Historical-Based Projections to 2100. *Geophys. Res. Lett.* **45**, 4248–4254, DOI: https://doi.org/10.1002/2017GL076649 (2018).

43. Casado, M., Orsi, A. J. & Landais, A. On the limits of climate reconstruction from water stable isotopes in polar ice cores. *Past Glob. Chang. Mag.* **25**, 146–147, DOI: 10.22498/pages.25.3.146 (2017).

44. Casado, M., Münch, T. & Laepple, T. Climatic information archived in ice cores: impact of intermittency and diffusion on the recorded isotopic signal in Antarctica. *Clim. Past* **16**, 1581–1598, DOI: 10.5194/cp-16-1581-2020 (2020).

45. Cox, P. M., Huntingford, C. & Williamson, M. S. Emergent constraint on equilibrium climate sensitivity from global temperature variability. *Nature* **553**, 319–322 (2018).

46. Schlund, M., Lauer, A., Gentine, P., Sherwood, S. C. & Eyring, V. Emergent constraints on equilibrium climate sensitivity in CMIP5: do they hold for CMIP6? *Earth Syst. Dyn.* **11**, 1233–1258 (2020).

47. Marshall, G. J., Fogt, R. L., Turner, J. & Clem, K. R. Can current reanalyses accurately portray changes in Southern Annular Mode structure prior to 1979? *Clim. Dyn.* **59**, 3717–3740, DOI: 10.1007/s00382-022-06292-3 (2022).

48. Jouzel, J. *et al.* Validity of the temperature reconstruction from water isotopes in ice cores. *J. Geophys. Res. Ocean.* **102**, 26471–26487, DOI: 10.1029/97JC01283 (1997).

49. Kino, K., Okazaki, A., Cauquoin, A. & Yoshimura, K. Contribution of the Southern Annular Mode to variations in water isotopes of daily precipitation at Dome Fuji, East Antarctica. *J. Geophys. Res. Atmospheres* **126**, e2021JD035397 (2021).

50. Servettaz, A. P. M. *et al.* Snowfall and water stable isotope variability in East Antarctica controlled by warm synoptic events. *J. Geophys. Res. Atmospheres* **125**, e2020JD032863 (2020).

51. Fogt, R. L. & Marshall, G. J. The Southern Annular Mode: variability, trends, and climate impacts across the Southern Hemisphere. *Wiley Interdiscip. Rev. Clim. Chang.* **11**, e652 (2020).

52. Fan, T., Deser, C. & Schneider, D. P. Recent Antarctic sea ice trends in the context of Southern Ocean surface climate variations since 1950. *Geophys. Res. Lett.* **41**, 2419–2426 (2014).

53. Steig, E. J. *et al.* Recent climate and ice-sheet changes in West Antarctica compared with the past 2,000 years. *Nat. Geosci.* **6**, 372–375 (2013).

54. Li, X. *et al.* Tropical teleconnection impacts on Antarctic climate changes. *Nat. Rev. Earth Environ.* **2**, 680–698, DOI: 10.1038/s43017-021-00204-5 (2021).

55. Lyu, K., Zhang, X., Church, J. A. & Hu, J. Evaluation of the interdecadal variability of sea surface temperature and sea level in the Pacific in CMIP3 and CMIP5 models. *Int. J. Climatol.* **36**, 3723–3740, DOI: https://doi.org/10.1002/joc.4587 (2016).

56. O'Reilly, C. H. *et al.* Projections of northern hemisphere extratropical climate underestimate internal variability and associated uncertainty. *Commun. Earth Environ.* **2**, 194, DOI: 10.1038/s43247-021-00268-7 (2021).

57. Ellerhoff, B. *et al.* Contrasting state-dependent effects of natural forcing on global and local climate variability. *Geophys. Res. Lett.* e2022GL098335 (2022).

58. DeConto, R. M. & Pollard, D. Contribution of Antarctica to past and future sea-level rise. *Nature* **531**, 591–597 (2016).

59. Garbe, J., Albrecht, T., Levermann, A., Donges, J. F. & Winkelmann, R. The hysteresis of the Antarctic ice sheet. *Nature* **585**, 538–544 (2020).

60. Reschke, M., Kunz, T. & Laepple, T. Comparing methods for analysing time scale dependent correlations in irregularly sampled time series data. *Comput. Geosci.* **123**, 65–72 (2019).

61. Rohde, R. *et al.* Berkeley Earth Temperature Averaging Process, Geoinfor. Geostat.-An Overview, 1, 2. *Geoinformatics Geostat. An Overv.* **1**, 20–100 (2013).

62. Osborn, T. J. & Briffa, K. R. The real color of climate change? *Science* **306**, 621–622 (2004).

63. Dansgaard, W. Stable isotopes in precipitation. *Tellus* **16**, 436–468, DOI: 10.1111/j.2153-3490.1964.tb00181.x (1964).

64. Lorius, C., Merlivat, L. & Hagemann, R. Variation in the mean deuterium content of precipitations in Antarctica. *J. Geophys. Res.* **74**, 7027–7031, DOI: 10.1029/JC074i028p07027 (1969).

65. Landais, A. *et al.* Surface studies of water isotopes in Antarctica for quantitative interpretation of deep ice core data. *Comptes Rendus Geosci.* (2017).

66. Masson-Delmotte, V. *et al.* A Review of Antarctic Surface Snow Isotopic Composition: Observations, Atmospheric Circulation, and Isotopic Modeling*. *J. Clim.* **21**, 3359–3387, DOI: 10.1175/2007JCLI2139.1 (2008).

67. Fujita, K. & Abe, O. Stable isotopes in daily precipitation at Dome Fuji, East Antarctica. *Geophys. Res. Lett.* **33**, DOI: 10.1029/2006GL026936 (2006).

68. Landais, A., Ekaykin, A., Barkan, E., Winkler, R. & Luz, B. Seasonal variations of 17O-excess and d-excess in snow precipitation at Vostok station, East Antarctica. *J. Glaciol.* **58**, 725–733, DOI: 10.3189/2012JoG11J237 (2012).

69. Touzeau, A. *et al.* Acquisition of isotopic composition for surface snow in East Antarctica and the links to climatic parameters. *The Cryosphere* **10**, 837–852, DOI: 10.5194/tc-10-837-2016 (2016).

70. Küttel, M., Steig, E. J., Ding, Q., Monaghan, A. J. & Battisti, D. S. Seasonal climate information preserved in West Antarctic ice core water isotopes: relationships to temperature, large-scale circulation, and sea ice. *Clim. Dyn.* **39**, 1841–1857, DOI: 10.1007/s00382-012-1460-7 (2012).

71. Buizert, C. *et al.* Antarctic surface temperature and elevation during the Last Glacial Maximum. *Science* **372**, 1097–1101 (2021).

72. Guillevic, M. *et al.* Spatial gradients of temperature, accumulation and δ 18 O-ice in Greenland over a series of Dansgaard–Oeschger events. *Clim. Past* **9**, 1029–1051 (2013).

73. Christiansen, B. & Ljungqvist, F. C. Challenges and perspectives for large-scale temperature reconstructions of the past two millennia. *Rev. Geophys.* **55**, 40–96, DOI: https://doi.org/10.1002/2016RG000521 (2017).

74. Freitas, A. C. M., Freitas, J. M. & Todd, M. Hitting time statistics and extreme value theory. *Probab. Theory Relat. Fields* **147**, 675–710 (2010).

75. Lucarini, V., Faranda, D. & Wouters, J. Universal behaviour of extreme value statistics for selected observables of dynamical systems. *J. statistical physics* **147**, 63–73 (2012).

76. Moloney, N. R., Faranda, D. & Sato, Y. An overview of the extremal index. *Chaos: An Interdiscip. J. Nonlinear Sci.* **29**, 22101 (2019).

77. Süveges, M. Likelihood estimation of the extremal index. *Extremes* **10**, 41–55 (2007).

Acknowledgements (not compulsory)

The results leading to these results has received funding from the DFG project CLIMAIC. The authors acknowledge the fruitful discussions with Thomas Laepple, Jilda A. Caccavo, Anais Orsi, and Cécile Agosta.

Author contributions statement

Must include all authors, identified by initials, for example: M.C. conceived the study and carried out the numerical surrogate data experiments, M.C. and D.F. applied the dynamical system theory to the system, M.C. and R.H. conceived the statistical and spectral approaches, M.C. led the redaction of the manuscript with the help of R.H.. All the authors discussed the results and contributed to the manuscript.

Methods

Datasets

We use the compilation of isotopic composition from ice core records from the PAGES working group Iso2k[35]. In Antarctica, this includes 78 records, most of which have an annual resolution, and amongst them, 15 cover more than 1000 years, as described in Stenni et al[29]. For the dynamical system framework, it is important that all the records have the same resolution, in order to avoid having a larger weight for the records with higher resolution. We homogenised the resolution of each records to annual resolution. For 16 of the records, the resolution was sub-annual (most of the time monthly), and we computed a block averaging to calendar years. For 6 of the records, the resolution was larger than one year, we resampled the records to annual resolution using a method inspired from Reschke et al[60]: we interpolated the data to a resolution of a tenth of a year, applied a Gaussian low pass filter to limit the impact of irregularities, and blocked average the record to annual resolution. This resampling approach limits both artifacts from the filter, and a small loss of information at high frequency[60]. The produced dataset includes then 78 records at annual resolution. The impact of the filtering does not affect the results.

The instrumental data is obtained via the database of station compiled for the Berkeley Earth Surface Temperature product[61], which comprises 24 time series, 11 of which begin as far back as 1958. In the case of CMIP5, we use eight past1000 simulations, which cover the period 850-1850, combined with historical simulations, which cover 1850-2005 (See supplementary Table S5). For CMIP6, as the past1000 simulations are not available yet, we compare the ice core results to the historical simulations (r*i*p1f*, 131 simulations) (See supplementary Table S6). For each simulation, we use the data from the gridpoints where ice core records are available in order to estimate (i) the trend of recent climate change between 1950 and 2005, (ii) the decadal variability (taken as the average power spectral density over the 5 - 40 years frequency band of the spectrum) after 1950 under strong anthropogenic forcing, and (iii) the natural decadal variability when anthropogenic forcing was still weak, prior to 1920. We include for comparison purposes the magnitude of anthropogenic warming and decadal variability obtained from the ice cores and converted into temperature with the most likely conversion factor (for Pan Antarctica, 0.5‰/°C, see Extended data ED6 and Methods) using estimates from both the statistical and dynamical frameworks.

Preparation of the stacked time series

We prepared regional and pan Antarctic stacks of the various datasets following a different approach than Stenni et al[29], where they create stack records using anomalies of isotopic composition against a common recent period (either 1960-1990 or 1900-1990), renormalise the variance of every independent time series, and use independent weights obtained from 3 different approaches for each time series to create their stacks. As we explain in the supplementary material, this approach might lead to biases because both the climatic signal and the archival noise[44] are renormalised to match the variance obtained in calibration time series[62].

Instead, we stack the anomaly of the records altogether without renormalising their variance independently. The common climatic signal will be unaffected, but the archival noises will be averaged out, and their relative contribution to the variance reduced by a factor N. The power spectral density (PSD) of the stack records then reflects mainly the spectrum of the climatic signal, and as a result, can be used to calibrate the stack as a temperature proxy more accurately[62]. We performed the anomaly for each time series independently against its total average value (no reference period) to avoid using a period affected by climate change as a reference period. While this approach could induce potential biases since the reference period for the different cores vary, sensitivity tests using only ice cores covering more than 1000 years (for which the anomaly calculation is mainly against pre-industrial period) show that the effects do not change the results. We then stack all the records to produce regional and pan-Antarctic time series. We use independent calibration between isotopic composition and temperature from the literature to convert the isotopic composition variability into temperature units (See next Method section).

We evaluated the impact of the very large number of cores in Dronning Maud Land for the reconstruction. Indeed, 31 of the 78 cores are located in a radius of 1000 km, leading to potentially an over-representation of this region in the stack. Follow Stenni et al (2017), we reproduce the results of this study taking into account only 3 cores from this region. At the scale of all of Antarctica, the two reconstructions are extremely well correlatated (r^2 = 0.89, $p < 0.005$, RMSE = 0.004), and similar results are obtained: a trend in isotopic composition between 1950 and 2005 of 0.14 ± 0.02 ‰/dec (instead of 0.11 ‰/dec when using all of the cores from the DML region). For the East Antarctica region, the reconstruction using only 3 cores from the DML region is also well correlated with the one using all the cores (r^2 = 0.70, $p < 0.005$, RMSE = 0.01), and we obtain a recent warming trend of 0.12 ± 0.04 ‰/dec (instead of 0.10 ‰/dec).

Overall, the stacking presented here leads to very similar reconstructions than the ones produced in Stenni et al[29], characterised by highly significant correlations (Supplementary, Section S1). The difference in the conclusions of our two studies arises from very different approaches used to evaluate the trends, both in the statistical and dynamical frameworks (Supplementary, Sections 4 and 5). To test the impact of the dropping number of cores after 2005, we computed the results of the manuscript taking into account only the cores covering at least the period from 1600 to 1990. The reconstruction using only these cores is well correlated with the one using all the cores (r^2 = 0.65, $p < 0.005$, RMSE = 0.24, see Supplementary Section S10).

Isotope to temperature calibration

Temperature reconstructions from water isotopes in ice cores are generally based on a linear relationship between isotopic composition and temperature[63,64]. While linear behaviour has been observed in numerous type of samples - spatially in the surface snow[65,66] - temporally in precipitation[12,67–69] - in surface snow[26] - in snowpit profiles[69,70] and in ice core records[71,72]; the obtained $\Delta\delta^{18}O/\Delta T$ slopes encompass a large range of values from 0.25 ‰$^{\circ}C^{-1}$ to

1.0 ‰°C^{-1}[43]. This was the motivation for Stenni et al[29] to mainly skip the conversion from isotope to temperature and display the results in units of $\delta^{18}O$.

A strong limitation from calibration directly on the ice core records using external temperature estimates (such as the borehole temperature, the $\delta^{15}N$, or meteorological observations over the recent period) is that the variance recorded by the water isotope record, which includes of both the climatic signal and the archival noise[26,27], is scaled to match the variance of the temperature estimates[62], which results in bias and artificial variance in the reconstructions[73], and more importantly for us, in an underestimation of the variability at low frequency[62]. In the case of ice core records in Antarctica, the archival noises (namely precipitation intermittency and stratigraphic noise) can impact the signal up to scales larger than centennial[28,44], and thus, lead to unrealistically high $\Delta\delta^{18}O/\Delta T$ slopes.

In order to avoid including archival noises, we evaluate spectrally the $\Delta\delta^{18}O/\Delta T$ slopes by comparing the regional iso2k stacks to regional ERA5 temperature timeseries. Indeed, we could remove the impact of the archival noise from the regional $\delta^{18}O$ stacks by comparing the average spectrum of all the n available records for a given region (100% of the archival noise is preserved) and the spectrum of the average timeseries where archival noise is averaged out and reduced proportionally to $\sqrt{n}$ following the approach detailed in Münch et al[28]. We additionally included the impact of isotopic diffusion and provide the spectra of the reconstructed temperature from the iso2k $\delta^{18}O$ stack for different values of $\Delta\delta^{18}O/\Delta T$ (see Extended Data Figure ED6 for Pan-Antarctica). The impact of diffusion mainly affect the interannual time scale for this stack, and as a result, do not yield significant impact on the calibration realised at the decadal scale (5 - 40 years window). The results support that the optimal calibration $\Delta\delta^{18}O/\Delta T$ slope to match ERA5 variability is 0.52 ‰°C^{-1} for Pan-Antarctica. This test was realised for each region where the signal to noise ratio was higher than two (See Supplementary), providing calibration slopes that are included in Extended Data Table ED1. Otherwise, the average value found for Antarctica (0.5 ‰°C^{-1}) was applied. The use of ERA5 data, despite their known biases, does not affect the calibration (see Supplementary Section S6).

The use of this spectral calibration provides much smaller error bars on the isotopic paleothermometer. Indeed, the range of values for the isotope to temperature conversion found in the literature are from 0.3 to 0.8 ‰°C^{-1}. For instance, to translate the warming trend obtained for the pan-Antarctic region of 0.11 ± 0.02‰/dec for the 1950 to 2005 period into temperature units, we would obtain a range of 0.14 to 0.30 °C/dec (Fig. 3). Instead, we obtain a value of 0.22 ± 0.04°C/dec (or a reduction of a factor of 2 of the error bar). In the dynamical framework, as the persistence diagnostic is independent from the unit of the time series (either ‰ or °C), we can avoid the conversion uncertainty and qualitatively compare the amplitude of the warming trend and natural variability in the iso2k stack with observations and the models.This supports that the isotope-to-temperature conversion for the Pan-Antarctica iso2k stack should be 0.5 ‰°C^{-1} or lower, which also constrains the warming trend range to [0.22 - 0.30]°C/dec.

Persistence

Climate proxies contain a large amount of information about the state of the underlying climate system. From a dynamical systems and statistical mechanics perspective, this implies that proxies are privileged observables of the system: not only do their values provide information on the underlying climate, but also their dynamical features, such as the persistence[32], are indicative of the underlying complex and chaotic dynamics. Small climate shifts or modest interdecadal variability could therefore be highlighted by dynamical systems metrics of persistence computed on proxy data. The persistence metric Θ describes the average residence time (in units of years for this study) of an observable of a natural system around a given state[33] (See Methods). In our case, the system that we investigate is the climate, and the observable, yearly Antarctic isotopic composition variations as a proxy of temperature at a given latitude-longitude. This means that very persistent states (such as red noise which can be used to mimic the climatic signal) yield values of Θ above one year and non-persistent states (such as pure white noise) yield values of Θ close to one year (See Methods). Higher values of Θ are associated with persistent and therefore more predictable states, or with a monotonous trend with a high signal-to-noise ratio (SNR) (Fig. 1 b). The persistence can thus be used as a dynamical constraint to identify a change of behaviour in a time series such as the emergence of the anthropogenic warming trend, or the reddening of the signal. To verify this hypothesis we compute the *persistence metric* Θ (in years) as a measure of the mean residence time of value in a time series around a given state. Θ is bounded to the range $\Theta > 1$. The larger the value of Θ, the more likely it is that the proxy time-series on the observations immediately preceding and following the chosen time will resemble the proxy time-series of that observation. On the other hand, when $\theta = 1$, the next and preceding proxy observation will be totally unrelated to the present one. We compute the persistence metric θ as follow. Given an ideally infinitely long proxy time series $x(t)$, and a proxy observation of interest ζ_x (one specific value), we define logarithmic returns as:

$$g(x(t), \zeta_x) = -\log[\text{dist}(x(t), \zeta_x)] \tag{1}$$

where *dist* is the Euclidean distance between two vectors. More generally, *dist* can be a distance function which tends to zero as the two vectors increasingly resemble each other. The $-\log$ implies that $g(x(t), \zeta_x)$ attains large values when $x(t)$ and ζ_x are close to one another. We thus have a time series g of logarithmic returns, which is large if x at a specific time resembles the state of interest ζ_x.

We next define a high threshold $s(q, \zeta_x)$ as the q*th* quantile of $g(x(t), \zeta_x)$ (here $q = 0.98$), and define exceedances $u(\zeta_x) = g(x(t), \zeta_x) - s(q, \zeta_x) \; \forall \; g(x(t), \zeta_x) > s(q, \zeta_x)$. These are effectively the so called Poincaré recurrences, for the chosen state ζ_x. We then leverage the Freitas-Freitas-Todd theorem[74,75], which states that the cumulative probability

distribution $F(u,\zeta)$ converges to the exponential member of the Generalised Pareto Distribution:

$$F(u,\zeta_x) \simeq \exp\left[-\vartheta(\zeta_x)\frac{u(\zeta_x)}{\sigma(\zeta_x)}\right] \tag{2}$$

Here, u and σ are parameters of the distribution which depend on the chosen ζ_x, while ϑ is the extremal index: the standard measure of clustering in extreme value theory[76]. We estimate the latter using the Süveges Maximum Likelihood Estimator[77]. We then obtain the persistence as: $\Theta(\zeta_x) = \Delta t/\vartheta(\zeta_x)$, where Δt is the timestep of the data being analysed, and the local dimension as $d(\zeta_x) = 1/\sigma(\zeta_x)$. The metrics' bounds are: $0 \leq d \leq +\infty$ and $1 \leq \Theta$. The persistence is calculated individually for each ice core series and then averaged over the entire Antarctic (Fig. 2a) and for the sub-regions, and is therefore free of weighting biases (Extended data Section S1).

Illustrations of how the persistence changes locally for a time series with realistic natural variability (characterised by a power law noise) and a trend occurring in the last section of the dataset are provided in Figures ED2, ED3, and ED4, as well as in Supplementary Section S3. To provide a rough correspondence between the observed changes of persistence and the amount of natural variability and the amplitude of the warming trend, we simulated an ensemble of 10 000 surrogate time series with varying scaling parameter (β), amount of decadal natural variability (average over the window 5 - 40 year), and trend magnitude and evaluated the ensemble of results that minimise the RMS error compared to the observations (Supplementary Section S4). Finally, we present the changes of the persistence Θ for different values of the decay time τ in the case of a first order auto-regressive process (AR1) or for power law noise for different values of β.

Trends

We calculate trends within a statistical framework by calculating a linear regression of the time series against the time axis. We evaluate the precision of the trends using surrogate data with similar spectral properties to the iso2k time series (scaling of 0.6 and matching decadal amplitude of natural variability) and a known trend of 0.1 ‰/dec (arbitrary choice of the same order of magnitude as the observations) applied for the last 50 years. We compared the measured trend with the actual input trend for 10 000 picks to evaluate the confidence interval of the trend estimator. We also used this approach to test the impact of the window length on the trend estimator (Supplementary Section S5).

We calculate trends within the dynamical system framework by using a Monte-Carlo simulation to obtain the magnitude of the persistence change for 10 000 simulations of random amplitude of natural variability (both changing the scaling β and the decadal variability amplitude) and magnitude of trend (Extended data Section S4).

Box plots

All error bars need to be defined in the legends (e.g. SD, SEM) together with a measure of centre (e.g. mean, median). For example, the legends should state something along the lines of “Data are presented as mean values +/- SEM” as appropriate. All box plots need to be defined in the legends in terms of minima, maxima, centre, bounds of box and whiskers and percentile.

Extended Data

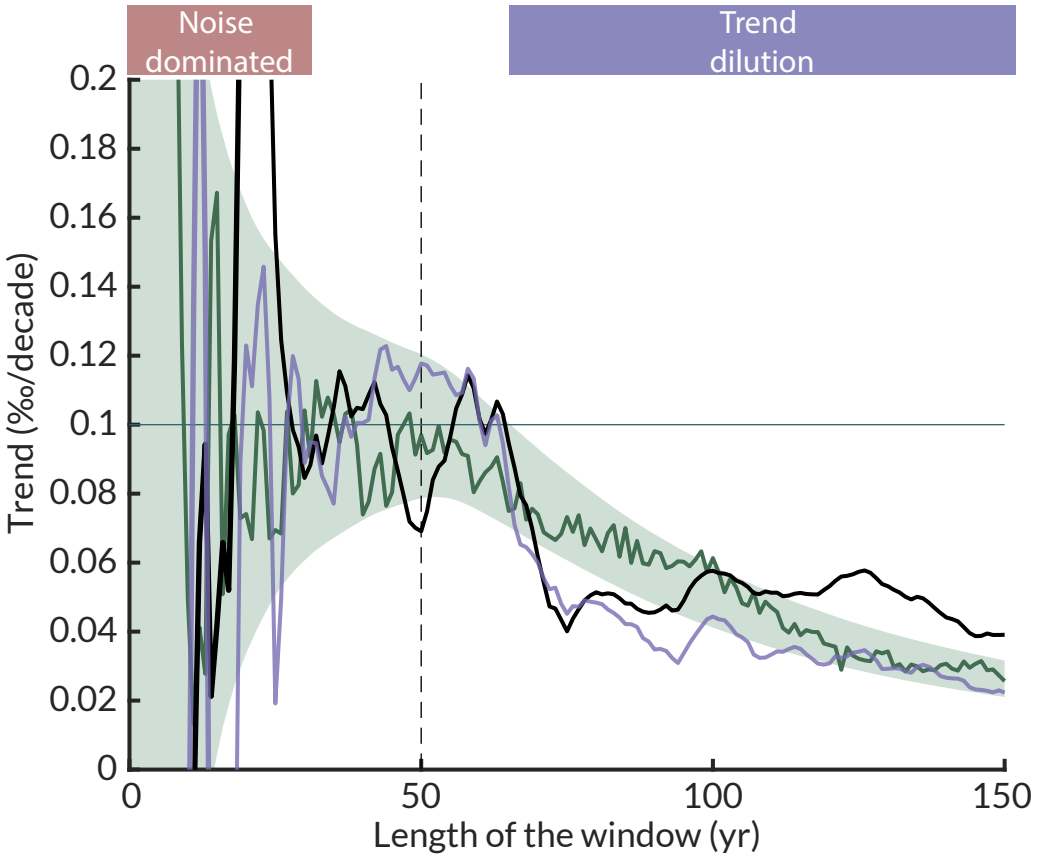

Figure ED1. Impact of window length on trend estimates: Iso2k stack for all of Antarctica (black), CPS reconstruction from Stenni et al,[29], and for an ensemble of 50 surrogate data simulated for realistic conditions in Antarctica (decadal natural variability of 0.6‰².yr, a beta of 0.6, and an amplitude of the anthropogenic warming of 0.1‰/dec starting 50 years prior to the end of the window over which the trend is calculated, see Supplementary Sections S2 and S3, dark green line), as well as confidence interval for an average of 50 cores calculated from 10 000 iterations (green shading).

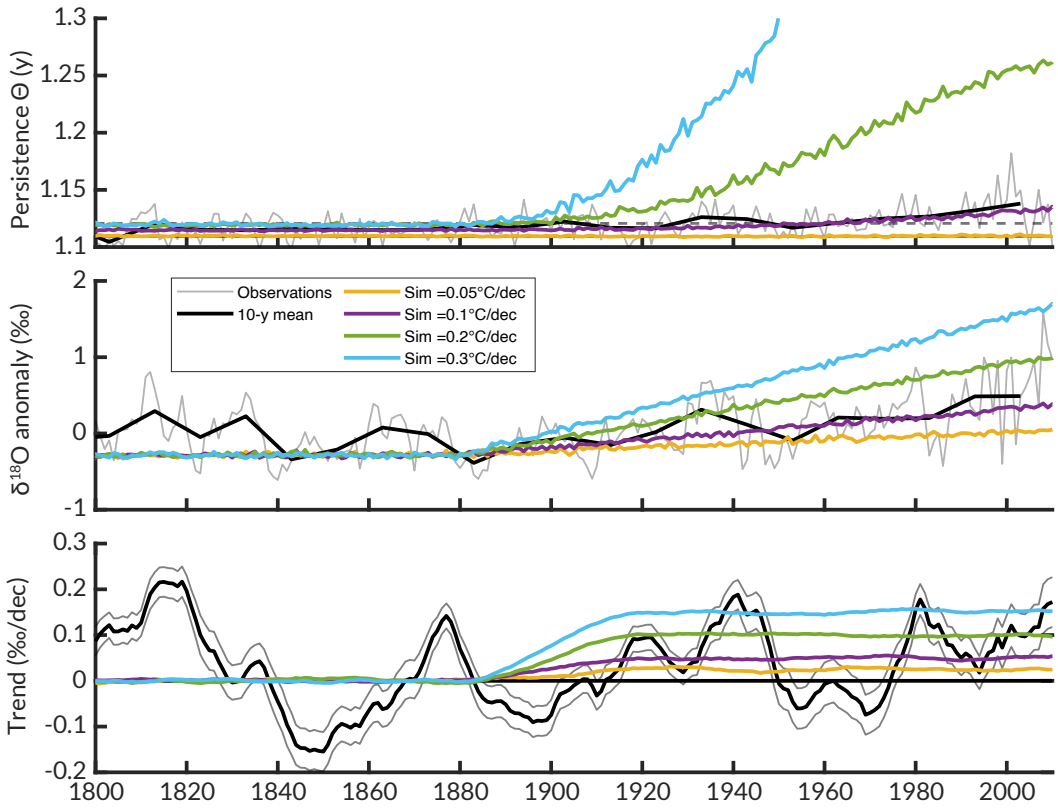

Figure ED2. Simulation of the trend impact on the persistence on surrogate data without any natural variability: change of persistence (Θ, top), $\delta^{18}O$ (middle), and 40-year running trend (bottom) as observed in the Iso2k stack (grey individual datapoints, black, 40-year block average) and for 4 different hypotheses on the intensity of the climatic change induced trend (from 0.05°C/dec to 0.3°C/dec, $\Delta\delta^{18}O \approx 0.5 \times \Delta T$)

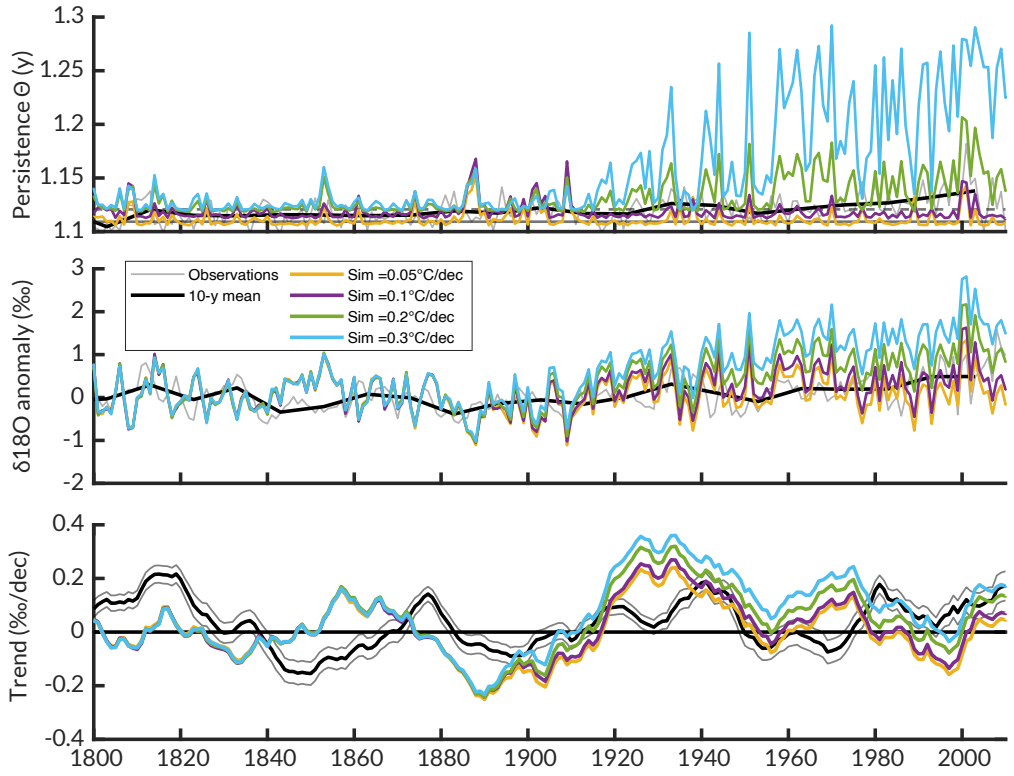

Figure ED3. Simulation of the trend impact on the persistence on surrogate data with natural variability: change of persistence (Θ, top), $\delta^{18}O$ (middle), and 40-year running trend (bottom) as observed in the Iso2k stack (grey individual datapoints, black, 40-year block average) and for 4 different hypotheses on the intensity of the climatic change induced trend (from 0.05°C/dec to 0.3°C/dec, $\Delta\delta^{18}O \approx 0.5 \times \Delta T$) with natural variability with a β of 0.6 and an average power at the decadal scale (10 – 40 years band) of 0.52‰²/y.

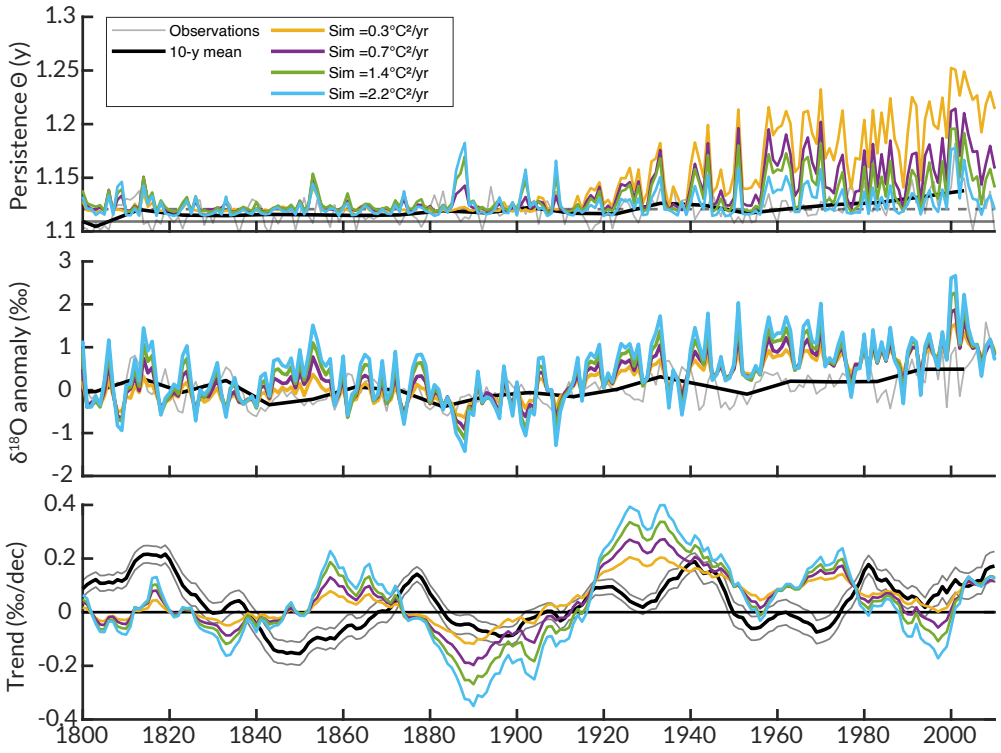

Figure ED4. Simulation of the natural variability and trend impact on the persistence on surrogate data:: change of persistence (Θ, top), $\delta^{18}O$ (middle), and 40-year running trend (bottom) as observed in the Iso2k stack (grey individual datapoints, black, 40-year block average) and for 4 different hypotheses on the intensity of the power of the natural variability with a β of 0.6 and average powers at the decadal scale (10 – 40 years band) ranging from 0.3 to 2.2 °C²/yr. The climate change induced trend is set to 0.2°C/dec ($\Delta\delta^{18}O \approx 0.5 \times \Delta T$).

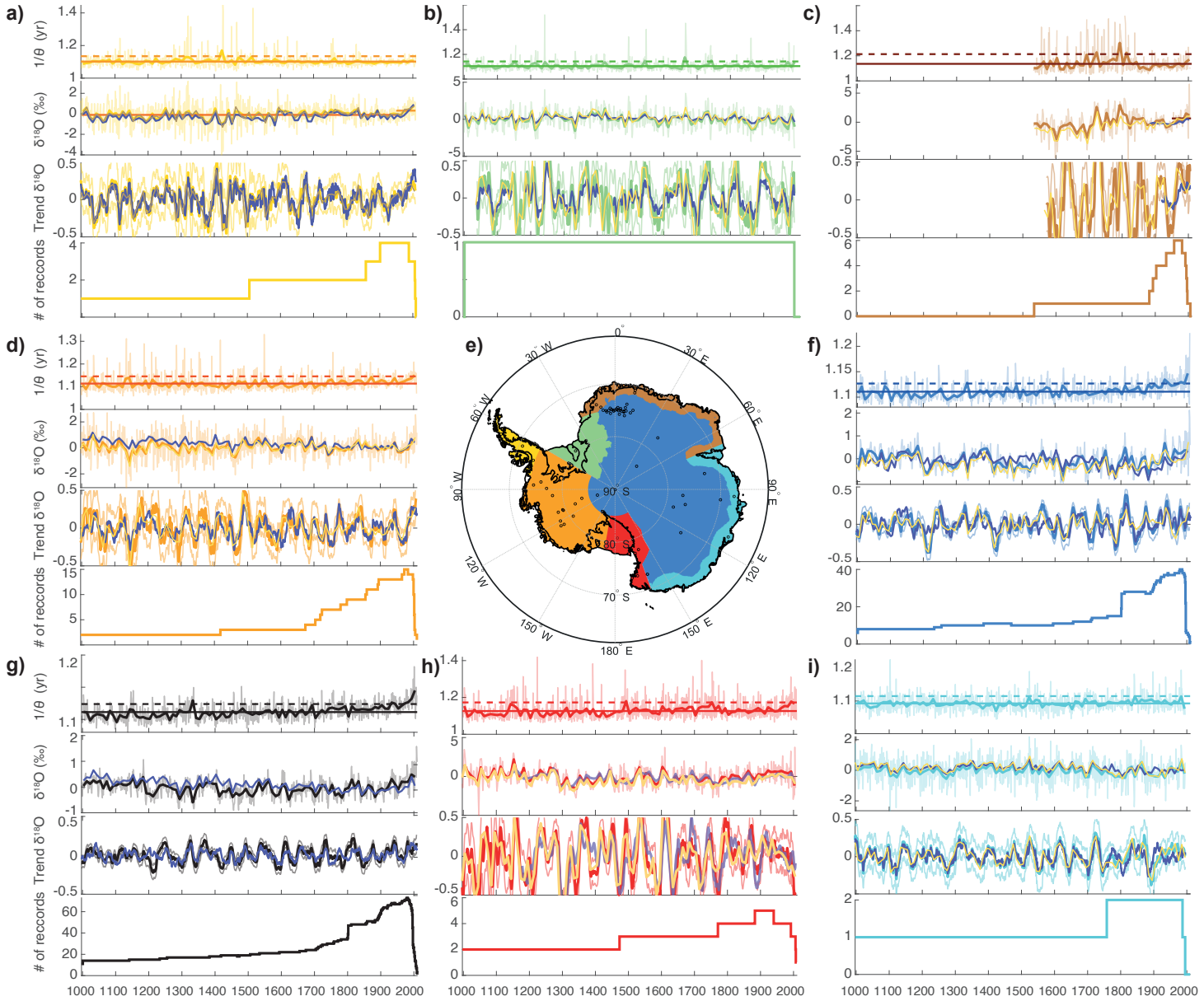

Figure ED5. Regional last 1000 years reconstructions: a) Antarctic Peninsula, b) Weddell Coast, c) Dronning Maud Land Coast, d) West Antarctica, e) map of the different regions, the black dots represent the station locations, f) East Antarctic Plateau, g) All of Antarctica, h) Victoria Land, and i) Indian Coast. For each panel, from top to bottom, time series of the persistence metric (Θ, y), isotopic composition anomaly stack for all ice cores in Antarctica (in δ^{18}O units ‰), compared to the previous stack realised by Stenni et al[29] (purple: CPS stack, yellow, unweighted stack, ‰), trend on 40-year running windows ending on the given year with confidence intervals, and number of records covering a given time period,. For Θ and δ^{18}O, light curves are the original data with annual resolution, thick curves are 10-year block averages. Note that the block averages and the trend estimates do not take into account datapoints after 2008 when the number of available cores drop below 10. For the top panel, the horizontal solid line represents the average value, while the horizontal dashed line is the average value +1 std.

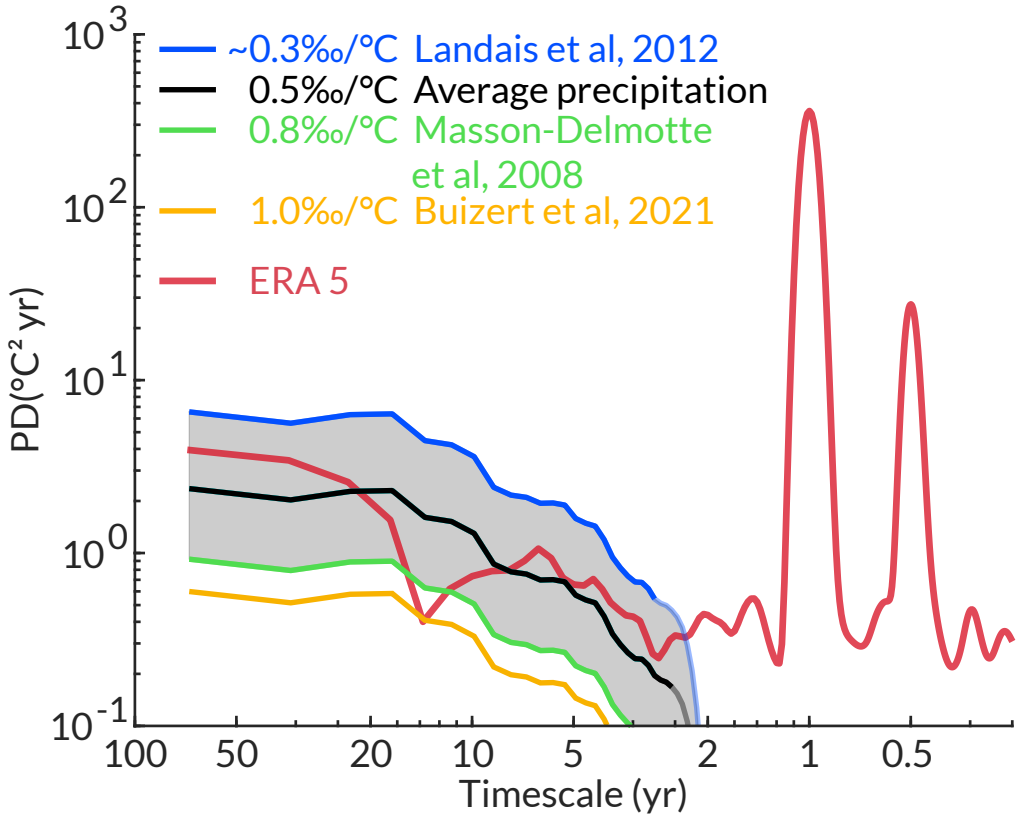

Figure ED6. Spectral constraint of the isotope-temperature calibration: power spectral density of the reconstructed temperature for different values of $\Delta\delta^{18}O/\Delta T$ between 1920 and 1990 compared to the spectrum of the ERA5 reanalysis outputs for the core location between 1951 and 2020 (the non-overlapping windows are set up to obtain the same length of time series with the largest number of cores; the results are insensitive to the window choice). The dip in ERA5 for timescales around 15 years is also found in the weather station observations and could be link to the SAM influence but was not taken into account for the sake of the calibration.

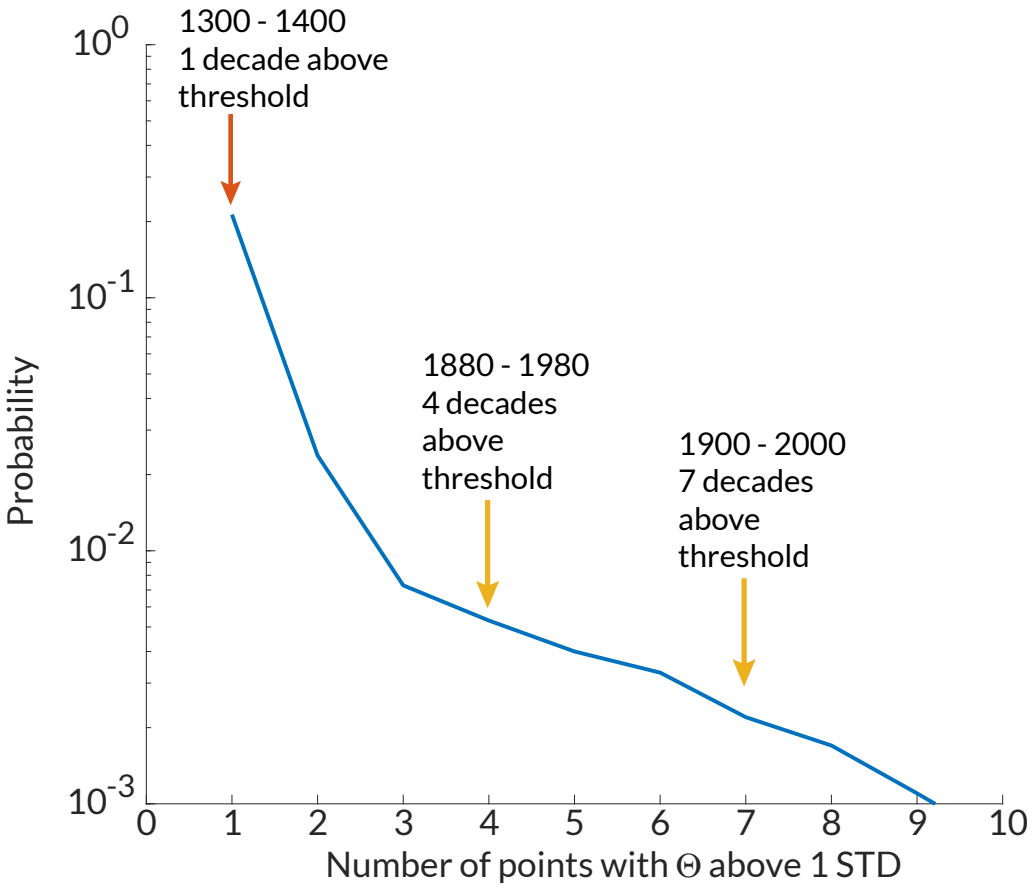

Figure ED7. Probability to obtain a given number of decades where Θ out of the range of values observed in the last 1000 years: Monte-Carlo analysis of the probability to obtain a given number of times when θ is above the confidence interval presented in Figure 2 (1 std on the whole time series) for a period of a 100 years using 10 000 iterations on the dataset.

Table ED1. Isotope to temperature calibration obtained for the different regions by spectral method. Regions for which the signal to noise ratio was not superior to 2 over a spectral range encompassing the one covered by ERA5 were not evaluated (NA), and the average Pan-Antarctica value was applied to them, as a best estimate.

Region	Isotope-Temperature calibration ($‰°C^{-1}$)
East Antarctica	0.49
Indian Coast	NA
Weddell Coast	NA
Peninsula	0.52
West Antarctica	0.69
Victoria Land	NA
DML	0.68
Pan-Antarctica	0.52